Available online at website: https://journal.bcrec.id/index.php/bcrec

Bulletin of Chemical Reaction Engineering & Catalysis, 20 (4) 2025, 624-630

Original Research Article

Charge Transport Kinetics in Fluorine-Doped Tin Oxide/Titanium Dioxide/Cadmium Sulfide/Cadmium Selenide Doped with Copper(II)/Zinc Sulfide Photoanode

Nguyen Van Minh[1], Nguyen Xuan Vinh[1*], Le Minh Nhan[2], Bui Van Thang[3], Deepu Thomas[4]

[1]Vinh Long University of Technology Education, Vinh Long Province, Vietnam.
[2]Department of Chemistry, Faculty of Basic Sciences, Can Tho University of Medicine and Pharmacy, Can Tho 94000, Vietnam.
[3]Dong Thap University, Dong Thap Province, Vietnam.
[4]Department of Physics, Nirmalagiri College, Nirmalagiri, 670701, India.

Received: 29th July 2025; Revised: 13th September 2025; Accepted: 13th September 2025
Available online: 22th September 2025; Published regularly: December 2025

Abstract

Quantum dot-sensitized solar cells face major limitations due to electron recombination, which reduces their overall efficiency. To address this challenge, we investigated copper-doped cadmium selenide as a novel approach to enhance charge transport in multilayer photoanodes. The objective of this study was to evaluate the effect of copper doping concentration on charge transport kinetics in TiO_2@CdS@CdSe:Cu^{2+}@ZnS photoanodes. Photoanodes with varying Cu contents (0–0.5 mol) were fabricated using the successive ionic layer adsorption and reaction method, followed by ZnS passivation. Electrochemical impedance spectroscopy and current–voltage characterization were employed to analyze charge transfer resistance, fill factor, power conversion efficiency, open-circuit voltage, and short-circuit current density. The optimized Cu(0.2) sample achieved the highest efficiency of 4.68% with a short-circuit current density of 27.35 mA/cm², attributed to improved charge transport, reduced recombination, and enhanced light absorption. However, excessive doping increased recombination and induced structural degradation. In conclusion, appropriate copper doping significantly improves the performance of QDSSCs, providing insights for designing advanced quantum absorber structures in next-generation solar cell technologies.

Keywords: Nanoscrystals; Quantum dot; Solar cell; High efficiency

How to Cite: Minh, N.V., Vinh, N.X., Nhan, L.M., Thang, B.V., Thomas, D. (2025). Charge Transport Kinetics in Fluorine-Doped Tin Oxide/Titanium Dioxide/Cadmium Sulfide/Cadmium Selenide Doped with Copper(II)/Zinc Sulfide Photoanode. *Bulletin of Chemical Reaction Engineering & Catalysis*, 20 (4), 624-630. (doi: 10.9767/bcrec.20455)

Permalink/DOI: https://doi.org/10.9767/bcrec.20455

1. Introduction

Dye-sensitized solar cells (DSSCs) have been extensively studied for decades, reaching efficiencies above 15% [1,2]. However, their performance is inherently limited by the Shockley–Queisser limit, primarily due to thermal energy losses and the restricted absorption range of dye molecules, which prevents full photon harvesting across the solar spectrum. To overcome these limitations, quantum dot-sensitized solar cells (QDSSCs) have been proposed as a promising alternative [3-6]. Quantum dots offer unique properties such as size-dependent band gaps, high absorption coefficients, and the ability to generate multiple excitons per photon. These features enable broader spectral absorption and improved conversion efficiency compared to conventional dye-based systems.

* Corresponding Author.
Email: vinhnx@vlute.edu.vn (N.X. Vinh)

Research on QDSSCs has demonstrated that incorporating nanocrystals such as CdS, CdSe, PbS, PbSe, and CdTe into photoanodes enhances light harvesting [7-11]. Nevertheless, the efficiency of single-quantum-dot systems remains constrained by their narrow absorption spectra. To address this issue, multilayer structures formed through methods like successive ionic layer adsorption and reaction (SILAR) and chemical bath deposition (CBD) have been developed. These approaches significantly improve current density and device efficiency. More recently, metal doping of nanocrystals has emerged as an effective strategy to introduce impurity energy levels within the band gap, thereby broadening absorption and enhancing charge transport. Reported examples include mercury doping in PbS, manganese doping in CdS/CdSe, copper doping in CdSe, and silver doping in CdSe, all of which achieved notable efficiency improvements. Despite these advances, previous studies have primarily focused on single-material doping and have not addressed the simultaneous co-doping of CdS and CdSe nanocrystals, which could further extend the absorption spectrum and maximize current density [12-14].

Another limitation in the current literature is the reliance on I–V characterization alone, which provides incomplete information about the internal mechanisms of QDSSCs. Parameters such as series resistance, recombination, and charge transport cannot be fully distinguished from I–V curves, as they can be fitted by multiple models. Electrochemical impedance spectroscopy (EIS), particularly when combined with I–V analysis, offers a more detailed evaluation of charge transfer, recombination, and ion diffusion processes. Although QDSSCs share structural similarities with DSSCs and can benefit from existing EIS models, their distinct features—such as quantum dot deposition techniques, counter electrode materials, and electrolyte compositions—necessitate tailored analysis [15-16].

While doping and multilayer structures have been shown to improve QDSSC performance, no study to date has systematically investigated the co-doping of CdS and CdSe nanocrystals within multilayer photoanodes. Furthermore, limited work has integrated I–V analysis with EIS modeling to provide a comprehensive understanding of charge transport dynamics in such systems. This paper addresses these gaps by introducing a novel Cu^{2+}-doped CdS/CdSe multilayer photoanode structure and by applying combined I–V and EIS characterization to extract key resistive parameters.

The objective of this work is to analyze the charge transport kinetics of Cu^{2+}-doped CdS/CdSe multilayer photoanodes using combined I–V and EIS techniques, in order to provide deeper insight into electron transfer, recombination, and transport mechanisms, and to demonstrate a pathway for enhancing the efficiency of QDSSCs.

2. Materials and Method

2.1 Fabrication of FTO/TiO_2/CdS/CdSe:Cu(0.3)/ZnS Photoanode and FTO/Cu_2S Cathode

The FTO/TiO_2 substrate was prepared by screen-printing a TiO_2 paste (Dyesol, 20 nm, anatase) and sintered at 500 °C for 30 min. The FTO@TiO_2@CdS:Cu(x) photoanodes (x = 0–0.5, molar ratio Cu^{2+}/Cd^{2+}) were fabricated via the SILAR method by sequential immersion in 0.1 M Cd^{2+} (from $Cd(CH_3COO)_2 \cdot 2H_2O$ in ethanol) and Cu^{2+} (from $CuCl_2$ in ethanol/water 1:1) for 5 min each, followed by ethanol washing. The films were then dipped in 0.1 M Na_2S (in water) at 60 °C for 5 min, washed with methanol, and dried at 120 °C for 15 min [17,18].

To prepare FTO@TiO_2@CdS@CdSe:Cu(0.3), the CdS:Cu(x) photoanodes were further immersed in 0.1 M Cd^{2+}/Cu^{2+} solution (Cu^{2+}/Cd^{2+} = 0.3), then in 0.3 M Se^{2-} solution (prepared from Se powder and Na_2SO_3 in NaOH) at 60 °C for 5 min. Three SILAR cycles were applied. A ZnS passivation layer was deposited via two SILAR cycles using 0.1 M Zn^{2+} (from $Zn(NO_3)_2$) and 0.1 M Na_2S, with 5 min immersion each.

QDSSCs were assembled using the synthesized photoanodes and FTO@Cu_2S counter electrodes, with an active area of 0.25 cm^2. The cells were filled with a polysulfide electrolyte (0.5 M Na_2S, 0.2 M S, 0.2 M KCl in DI water) and tested under ~100 $mW.cm^{-2}$ illumination (Figure 1).

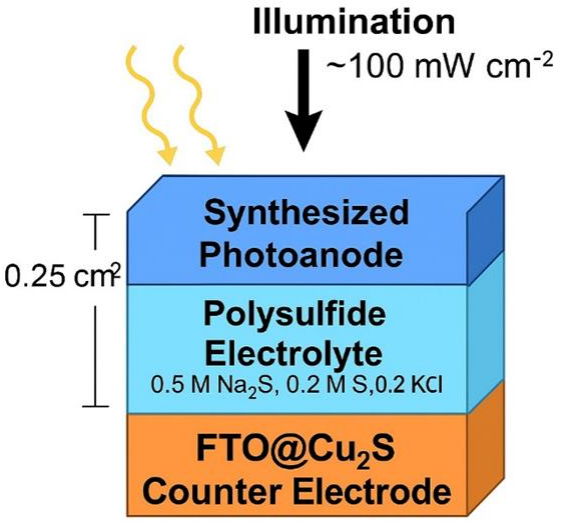

Figure 1. The structure of QDSSCs.

2.2 Characterizations

The characterization of photoanodes and QDSSCs is facilitated by several instruments: an electroluminescence spectrophotometer for measuring total photoluminescence of various materials; the Interface 5000E electrochemical workstation for analyzing kinetic mechanisms within QDSSCs; and the Keithley 2450 photovoltaic system for evaluating power conversion efficiency.

3. Results and Discussion

Both R_S and R_{SH} are independent of light intensity and voltage. Additionally, there is dynamic resistance, which depends on the voltage and is determined using dynamic modeling under dark conditions. The relationship among the photocurrent (I_{ph}), diffusion current (I_d), and load current (I_L) can be determined under three different operating conditions (Figure 2).
Open-circuit voltage condition:

$$I_{ph} = I_d + I_{SH} \quad (1)$$

$$I_{ph} = I_o(e^{\alpha V_{OC}} - 1) + \frac{V_{OC}}{R_{SH}} \quad (2)$$

With $\alpha = \frac{q}{nkT}$.

Short-circuit current condition:

$$I_{ph} = I_d + I_{SH} + I_{SC} \quad (3)$$

$$I_{ph} = I_o(e^{\alpha I_{SC} R_S} - 1) + \frac{I_{SC} R_S}{R_{SH}} + I_{SC} \quad (4)$$

Condition for having a conductor:

$$I_{ph} = I_d + I_{SH} + I_L \quad (5)$$

$$I_{ph} = I_o\left(e^{\alpha(V_L + I_L R_S)} - 1\right) + \frac{V_L + I_L R_S}{R_{SH}} + I_L \quad (6)$$

At any two points (V_1,I_1) and (V_2,I_2) on an I-V curve, the relationship between V and I is given as follows:

$$V_1 = \frac{1}{\alpha} ln\left[\frac{R_{SH}(I_{ph} + I_o - I_1)}{R_{SH} I_o} - I_1 R_S\right] - I_1 R_S \quad (7)$$

$$V_2 = \frac{1}{\alpha} ln\left[\frac{R_{SH}(I_{ph} + I_o - I_2)}{R_{SH} I_o} - I_2 R_S\right] - I_2 R_S \quad (8)$$

From (8) and (9), we obtain the expression R_S:

$$R_S = \frac{V_1 - V_2}{I_2 - I_1} - \frac{1}{\alpha(I_2 - I_1)} ln\left[\frac{R_{SH}(I_{ph} + I_o - I_1) - I_1 R_S}{R_{SH}(I_{ph} + I_o - I_2) - I_2 R_S}\right] \quad (9)$$

Normally, R_{SH} is much larger than R_S, therefore $R_{SH}(I_{ph} + I_o - I_1) \gg I_1 R_S$; $R_{SH}(I_{ph} + I_o - I_2) \gg I_2 R_S$:

$$R_S = \frac{V_1 - V_2}{I_2 - I_1} - \frac{1}{\alpha(I_2 - I_1)} ln\left[\frac{I_{ph} + I_o - I_1}{I_{ph} + I_o - I_2}\right] = R_D - R_d \quad (10)$$

With:

$$R_D = \frac{V_1 - V_2}{I_2 - I_1} \quad (11)$$

$$R_d = \frac{1}{\alpha(I_2 - I_1)} ln\left[\frac{I_{ph} + I_o - I_1}{I_{ph} + I_o - I_2}\right] \quad (12)$$

R_D and R_d are the external and internal dynamic resistances of the photovoltaic module. The parallel resistance obtained from the above expressions is:

$$R_{SH} = \frac{V_{OC}}{I_{ph} - I_o(e^{\alpha V_o} - 1)} \quad (13)$$

Additionally, R_S can also be determined based on the I–V curve under dark conditions:

$$R_S = -\frac{V_1 - V_2}{I_2 - I_1} + \frac{1}{\alpha(I_2 - I_1)} ln\left[\frac{I_o - I_1}{I_o - I_2}\right] = R_d - R_D \quad (14)$$

The data from solar cell samples doped with different concentrations of Cu (0, 0.1, 0.2, 0.3, 0.5) and having the structure TiO_2@CdS@CdSe show notable variations in performance metrics such as power conversion efficiency (PCE), fill factor (FF), open-circuit voltage (V_{oc}), and short-circuit current density (J_{sc}). When Cu is added at concentrations of 0.1 or more, the V_{oc} value, which was first measured at 0.48 V for the undoped sample, slightly rises to 0.5 V and stays constant at higher doping levels (Figure 3). This suggests

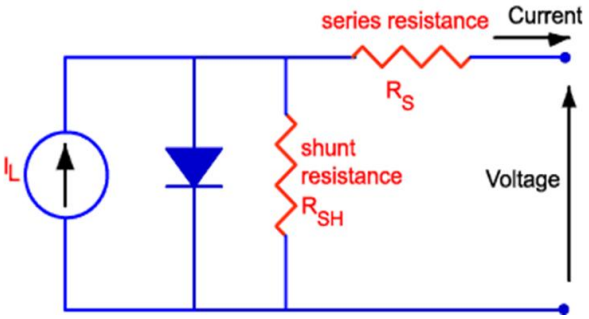

Figure 2. The equivalent circuit diagram of QDSSCs [19-22].

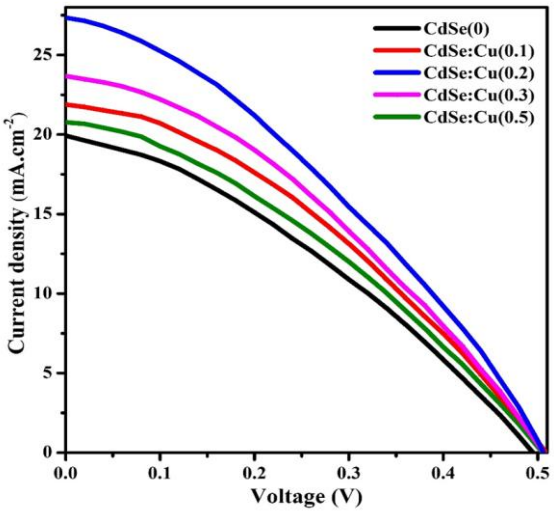

Figure 3. The PCE of QDSSCs.

that Cu doping could increase the device's open-circuit voltage by lowering electron recombination at the interface. With respect to J_{sc}, the current density rises from 19.9 mA/cm² in the undoped sample to a maximum of 27.35 mA/cm² in the Cu(0.2) sample. At Cu concentrations of 0.3 and 0.5, respectively, the current density progressively falls to 23.68 and 20.77 mA/cm². This implies that while higher Cu levels may cause crystal defects or increase charge recombination, which would negatively impact current generation, low-level Cu doping (0.1–0.2) may improve light absorption or increase charge transport efficiency. FF exhibits a comparable pattern. At low Cu concentration, the Cu(0.1) sample shows the highest FF value of 0.3813, indicating better electrical contact and lower internal resistance. However, FF drops to 0.3523 (Cu 0.2), 0.3478 (Cu 0.3), and 0.3471 (Cu 0.5) as the Cu content rises. This could be a result of detrimental effects on contact loss or internal resistance. When these three parameters are combined, the PCE rises from 3.31% (Cu 0) to a peak of 4.68% at Cu(0.2), after which it falls to 4.42% and 3.61% at Cu(0.3) and Cu(0.5), respectively. With a balanced combination of Voc, Jsc, and FF, the TiO_2@CdS@CdSe:Cu(0.2) sample is found to be optimal, resulting in the best overall performance. Excessive doping may be the cause of the decrease in PCE at higher Cu doping levels since it can weaken the crystal structure or increase the density of surface defects [23-25].

The aforementioned analysis indicates that, when properly managed, doping Cu into the TiO_2@CdS@CdSe system significantly enhances the performance of QDSSCs. For maximum efficiency, a Cu content of 0.2 seems to be ideal. However, because of increased recombination and structural degradation, performance may suffer if this threshold is exceeded. Therefore, it is essential to precisely control Cu doping during material synthesis in order to maximize device performance. An essential foundation for the creation of more effective quantum absorber structures in upcoming solar cell technologies is provided by this analysis.

Based on a single lighted I–V curve, a photovoltaic device's dynamic resistance under illumination can be divided into R_D and R_d. Previous research have established a QDSSCs dynamic resistance technique [22]. Figure 2 shows the equivalent circuit of the solar cell and the relationships between I_{ph}, I_d, and I_L under three operating circumstances, including open-circuit.

The resistance values in Table 1 were computed using Equations 7, 8, and 9 from a single I-V curve. The findings indicate that the resistance values were influenced by the QDs films' thickness. We can examine and assess the resistance parameters of QDSSCs with various quantum dot structures of TiO_2@CdS@CdSe doped with different concentrations of Cu based on the data table. The undoped sample (Cu(0)) has the highest interfacial resistance (I_O) (1.75×10^{-6} Ω/cm²), which leads to a relatively high external resistance (R_D = 66.67 Ω) and internal resistance (R_d = 1850 Ω). I_O dramatically drops to 8.87×10^{-8} Ω/cm² when Cu is added at a concentration of 0.1 mol, but this causes a significant increase in R_d (3390 Ω) and R_D (121.7 Ω), suggesting a dual-effect behavior: Cu enhances charge transport at the surface but also raises internal resistance because of Cu–quantum dot interactions. Relative stability is indicated by the slight fluctuations in the parameters I_O, R_d, and R_D at Cu concentrations of 0.2–0.3 mol. In particular, R_d is roughly 2790–2810 Ω, R_D is roughly 100 Ω, and I_O is between $(1.11–0.96)\times10^{-7}$ Ω/cm². Between 2690 and 2710 Ω·cm², R_S exhibits a slight decrease, indicating that Cu doping at this level preserves the best possible charge transport in the external circuit. Notably, I_O drops to 8.42×10^{-8} Ω/cm² at a Cu concentration of 0.5 mol, the lowest of all samples, but R_d (5410 Ω) and R_D (200 Ω) sharply increase at the same time. This suggests an overdoping effect, which prevents charge transport because of increased electron-hole recombination in the substance [26-29].

The Cu(0.2) sample exhibits the highest value of R_{SH}, a crucial parameter associated with leakage current losses (27.35 kΩ·cm²), indicating its superior ability to suppress leakage current.

Table 1. Parameters of the QDSSCs are calculated using the two-point method based on the solar cell's efficiency.

Samples	I_O (Ω/cm²)	R_d(Ω)	R_D(Ω)	R_S (Ω.cm²)	R_{SH} (kΩ.cm²)
TiO_2@CdS@CdSe:Cu(0)	1.75×10^{-6}	1850	66.67	1780	19.9305
TiO_2@CdS@CdSe:Cu(0.1)	8.87×10^{-8}	3390	121.7	3270	21.8929
TiO_2@CdS@CdSe:Cu(0.2)	1.11×10^{-7}	2790	100.2	2690	27.3502
TiO_2@CdS@CdSe:Cu(0.3)	9.6×10^{-8}	2810	100	2710	23.6812
TiO_2@CdS@CdSe:Cu(0.5)	8.42×10^{-8}	5410	200	5210	20.7712

Therefore, TiO_2@CdS@CdSe:Cu(0.2) has the most balanced resistance parameters of all the samples that were studied, which helps the QDSSC device operate at its best.

QDSSC kinetic processes are studied using electrochemical impedance spectra from five Cu-doped CdS nanocrystal concentrations. After measurement, the experimental spectrum is fitted to the QDSSC circuit model to determine R_{ct1} and R_{ct2}. The R_{ct1} resists electron diffusion in the Cu_2S cathode and electrolyte surface. The resistance to charges transfer between the TiO_2/nanocrystals surface and diffusion in the TiO_2 film is R_{ct2}. Table 1 and Figure 4 show that smaller resistance values reduce recombination losses and increase current density. Table 1 and Figure 4 reveal that the R_{ct2} and R_{ct1} resistances of 0.2 Cu doped QDSSCs using FTO@TiO_2@CdS@CdSe:Cu(0.3)@ZnS electrodes are the lowest at 24.78 Ω and 10.58 Ω, respectively, compared to other Cu concentrations. Due of the quick electron transition between TiO_2, nanocrystals, and Cu_2S films and surfaces, this filling reduces electron assembly processes. The sharp increase in J_{sc} of 27.3501 mA.cm^{-2} reflects this outcome. Cu doping in CdS boosts light harvesting, generation, collecting, and injection in QDSSCs, as seen by the absorption spectra, which is substantially enhanced compared to Phat *et al.* [18]. R_{ct2} and R_{ct1} increase with Cu doping concentrations above or below 0.2. At doping doses of 0 and 0.1, R_{ct2} resistance values of 186.4 Ω and 143.2 Ω are observed. Because Cd has a higher resistance than Cu in CdS and CdSe:Cu^{2+} films. At Cu doping concentrations larger than 0.2, the absorption spectra results match this conclusion. High concentration doping makes the CdSe:Cu^{2+} film non-homogeneous, causing agglomeration and bigger particles. The results of this study match with result of Mohammed *et al*. where the authors doped Cu into CdS in QDSSCs with a TiO_2@CdS electrode to extend the absorption peak and increase conversion efficiency [30-34].

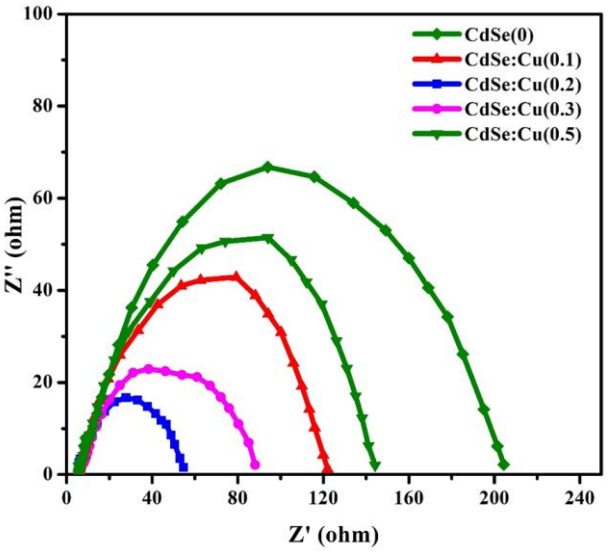

Figure 4. EIS spectrum of QDSSCs.

4. Conclusions

This study demonstrates that controlled Cu^{2+} doping in TiO_2@CdS@CdSe@ZnS photoanodes plays a decisive role in charge transport kinetics and photovoltaic performance of QDSSCs. The optimal doping concentration at x = 0.2 yielded the highest power conversion efficiency (4.68%), improved charge transfer, enhanced light absorption, and reduced recombination, advancing current understanding of dopant engineering in nanostructured photoanodes. Conversely, excessive doping ($x \geq 0.3$) induced structural defects and higher resistance, leading to efficiency loss. These findings provide clear guidance for the rational design of high-efficiency QDSSC photoanodes, thereby contributing valuable insight to the future development of next-generation solar energy devices.

Acknowledgments

The authors wish to express the colleagues for providing the resources and support needed to complete this study.

CRedit Author Statement

Author Contributions: Nguyen Van Minh: Writing Draft Preparation, Visualization, Resources, Methodology, Formal Analysis; Nguyen Xuan Vinh: Methodology, Formal Analysis, Data Curation, Review and Editing; Le

Table 2. Parameters characterizing of the QDSSCs.

Samples	V_{oc} (V)	J_{sc} (mA.cm^{-2})	FF	PCE (%)	R_{ct1} (Ω)	R_{ct2} (Ω)
TiO_2@CdS@CdSe:Cu(0)	0.48	19.9	0.345	3.3	12.04	186.4
TiO_2@CdS@CdSe:Cu(0.1)	0.5	21.89	0.381	3.96	11.08	143.2
TiO_2@CdS@CdSe:Cu(0.2)	0.5	27.35	0.352	4.68	10.58	24.78
TiO_2@CdS@CdSe:Cu(0.3)	0.5	23.68	0.348	4.42	10.88	55.56
TiO_2@CdS@CdSe:Cu(0.5)	0.5	20.77	0.347	3.61	11.32	153.2

Minh Nhan, Bui Van Thang and Deepu Thomas: Methodology, Investigation. All authors have read and agreed to the published version of the manuscript.

References

[1] Hu, Y., Shan, Y., Yu, Z., Sui, H., Qiu, T., Zhang, S., Ruan, W., Xu, Q., Jiao, M., Wang, D., Wu, Y. (2022). Incorporation of γ-aminobutyric acid and cesium cations to formamidinium lead halide perovskites for highly efficient solar cells. *Nano Energy,* 64, 561–567. DOI: 10.1016/j.jechem.2021.05.025

[2] Luo, D., Li, L., Shi, Y., Zhang, J., Wang, K., Guo, X., Kyaw, A.K.K. (2021). Electron-deficient diketone unit engineering for non-fused ring acceptors enabling over 13% efficiency in organic solar cells. *Journal of Materials Chemistry A,* 9(26), 14948–14957. DOI: 10.1039/D1TA03643B

[3] Rühle, S., Shalom, M., & Zaban, A. J. (2010). Quantum-dot-sensitized solar cells. *ChemPhysChem,* 11(11), 2290–2304. DOI: 10.1002/cphc.201000069

[4] Cohn, A.W., Schimpf, A.M., Gunthardt, C.E., Gamelin, D.R. (2013). Size-dependent trap-assisted Auger recombination in semiconductor nanocrystals. *Nano Letters,* 13(4), 1810–1815. DOI: 10.1021/nl400503s

[5] Zhang, Y., Liu, J., Li, S.-L., Su, Y.-M., Lan, Y.-Q. (2019). Polyoxometalate-based materials for sustainable and clean energy conversion and storage. *EnergyChem, 1*(3), 100021. DOI: 10.1016/j.enchem.2019.100021

[6] Tian, J., Zhang, Q., Uchaker, E., Gao, R., Qu, X., Zhang, S., Cao, G. (2013). Architectured ZnO photoelectrode for high efficiency quantum dot sensitized solar cells. *Energy & Environmental Science,* 6(12), 3542–3547. DOI: 10.1039/C3EE41056K

[7] Bang, J.H., Kamat, P.V. (2009). Quantum dot sensitized solar cells. A tale of two semiconductor nanocrystals: CdSe and CdTe. *ACS Nano, 3*(6), 1467–1476. DOI: 10.1021/nn900324q

[8] González-Pedro, V., Shen, Q., Jovanovski, V., Giménez, S., Tena-Zaera, R., Toyoda, T., Mora-Seró, I. (2013). Ultrafast characterization of the electron injection from CdSe quantum dots and dye N719 co-sensitizers into TiO_2 using sulfide based ionic liquid for enhanced longterm stability. *Electrochimica Acta,* 100, 35–43. DOI: 10.1016/j.electacta.2013.03.119

[9] Schaller, R.D., Klimov, V.I. (2004). High efficiency carrier multiplication in PbSe nanocrystals: Implications for solar energy conversion. *Physical Review Letters,* 92(18), 186601. DOI: 10.1103/PhysRevLett.92.186601

[10] Hara, K., Sayama, K., Ohga, Y., Shinpo, A., Suga, S., Arakawa, H. (2018). A Coumarin-derivative dye-sensitized nanocrystalline TiO_2 solar cell having a high solar energy conversion efficiency up to 5.6 percent. *Renewable Energy*, 2, 214–218. DOI: 10.1039/B010058G

[11] Sun, J.-K., Jiang, Y., Zhong, X., Hu, J.-S., Wan, L.-J. (2017). Three-dimensional nanostructured electrodes for efficient quantum-dot-sensitized solar cells. *Nano Energy,* 32, 130–156. DOI: 10.1016/j.nanoen.2016.12.022

[12] Pawar, S.A., Patil, D.S., Jung, H.R., Park, J.Y., Mali, S.S., Hong, C.K., Shin, J.-C., Patil, P.S., Kim, J.-H. (2016). Quantum dot sensitized solar cell based on TiO_2/CdS/CdSe/ZnS heterostructure. *Electrochimica Acta,* 203, 74–83. DOI: 10.1016/j.electacta.2016.04.029

[13] Zhang, Y., Zhu, J., Yu, X., Wei, J., Hu, L., Dai, S. (2012). The optical and electrochemical properties of CdS/CdSe co-sensitized TiO_2 solar cells prepared by successive ionic layer adsorption and reaction processes. *Solar Energy,* 86(3), 964–971. DOI: 10.1016/j.solener.2012.01.006

[14] Zhou, R., Zhang, Q., Uchaker, E., Lan, J., Yin, M., Cao, G. (2014). Mesoporous TiO_2 beads for high efficiency CdS/CdSe quantum dot co-sensitized solar cells. *ACS Applied Materials & Interfaces,* 2(8), 2517–2525. DOI: 10.1039/C3TA13460A

[15] Mora-Sero, I., Giménez, S., Fabregat-Santiago, F., Gómez, R., Shen, Q., Toyoda, T., Bisquert, J. (2009). Recombination in quantum dot sensitized solar cells. *Accounts of Chemical Research,* 42(11), 1848–1857. DOI: 10.1021/ar900134d

[16] Dai, Qilin, Erwin M. Sabio, Wenyong Wang, and Jinke Tang (2014). Pulsed laser deposition of Mn doped CdSe quantum dots for improved solar cell performance. *Applied Physics Letters,* 104(18). DOI: 10.1063/1.4875107

[17] Thao, N.T., Phuong, H.N., Tung, H.T., Phat, N.T., Dat, H.T., Vinh, L.Q. (2018). The enhanced current density of the quantum dots solar cells based on CdSe:Mn^{2+} crystalline. *Optical Materials,* 84, 199–204. DOI: 10.1016/j.optmat.2018.06.069

[18] Nguyen, T.P., Ha, T.T., Nguyen, T.T., Ho, N.P., Huynh, T.D., Lam, Q.V. (2018). Effect of Cu^{2+} ions doped on the photovoltaic features of CdSe quantum dot sensitized solar cells. *Electrochimica Acta, 282,* 16–23. DOI: 10.1016/j.electacta.2018.06.046

[19] Yang, J., Mei, S., & Ferreira, J. M. (2002). Hydrothermal synthesis of well-dispersed TiO_2 nano-crystals. *Journal of Materials Research,* 17(9), 2197–2200. DOI: 10.1557/JMR.2002.0323

[20] Shen, Q., Kobayashi, J., Diguna, L.J., Toyoda, T. (2008). Effect of ZnS coating on the photovoltaic properties of CdSe quantum dot-sensitized solar cells. *Journal of Applied Physics,* 103(8). DOI: 10.1063/1.2903059

[21] Ebothé, J., Michel, J., Kityk, I.V., Lakshminarayana, G., Yanchuk, O.M., Marchuk, O.V. (2018). Influence of CdS nanoparticles grain morphology on laser-induced absorption. *Physica E,* 100, 69–72. DOI: 10.1016/j.physe.2018.03.002

[22] Thanh, T. H., Quang, V. L., & Thanh, D. H. (2015). Determination of the dynamic resistance of the quantum dots solar cells by one I–V curve and electrochemical impedance spectra. *Solar Energy Materials and Solar Cells,* 141, 167–172. DOI: 10.1016/j.solmat.2015.07.007

[23] Sun, J.K., Jiang, Y., Zhong, X., Hu, J. S., Wan, L. J. (2017). Three-dimensional nanostructured electrodes for efficient quantum-dot-sensitized solar cells. *Nano Energy*, 32, 130-156. DOI: 10.1016/j.nanoen.2016.12.022

[24] Li, C., Yang, L., Xiao, J., Wu, Y.-C., Søndergaard, M., Luo, Y., Li, D., Meng, Q., Iversen, B.B. (2013). ZnO nanoparticle based highly efficient CdS/CdSe quantum dot-sensitized solar cells. *Physical Chemistry Chemical Physics,* 15*(22),* 8710–8715. DOI: 10.1039/C3CP50365H

[25] Hsu, Y.J., Lu, S.Y., Lin, Y.F. (2005). One-step preparation of coaxial CdS–ZnS and $Cd_{1-x}Zn_xS$–ZnS nanowires. *Advanced Functional Materials,* 15*(8),* 1350–1357. DOI: 10.1002/adfm.200400563

[26] Klimov, V.I., Mikhailovsky, A.A., Xu, S., Malko, A., Hollingsworth, J.A., Leatherdale, A.C.A., Eisler, H.-J., Bawendi, M.G. (2000). Optical gain and stimulated emission in nanocrystal quantum dots. *Science,* 290(5490), 314–317. DOI: 10.1126/science.290.5490.314

[27] Roy, A., Mohamed, M.J.S., Gondal, M.A., Mallick, T.K., Tahir, A.A., Sundaram, S. (2023). Co-sensitization effect of N719 dye with Cu doped CdS colloidal nanoparticles for dye sensitized solar cells. *Inorganic Chemistry Communications,* 148, 110298. DOI: 10.1016/j.inoche.2022.110298

[28] Tarimo, D.J., Oyedotun, K.O., Mirghin, A., Sylla, N.F., Manyala, N. (2022). Asymmetric ultracapacitor produced by sulphur reduced graphene oxide/metal oxide composite with high energy density and outstanding cycling. In *Electrochemical Society Meeting Abstracts* (Vol. 242). The Electrochemical Society, Inc. DOI: 10.1149/MA2022-02169mtgabs

[29] Hou, J., Zhao, H., Huang, F., Jing, Q., Cao, H., Wu, Q., Peng, S., Cao, G. (2016). High performance of Mn-doped CdSe quantum dot sensitized solar cells based on the vertical ZnO nanorod arrays. *Journal of Power Sources,* 325*,* 438–445. DOI: 10.1016/j.jpowsour.2016.06.070

[30] Zhang, C., Liu, S., Liu, X., Deng, F., Xiong, Y., Tsai, F.-C. (2018). Incorporation of Mn^{2+} into CdSe quantum dots by chemical bath co-deposition method for photovoltaic enhancement of quantum dot-sensitized solar cells. *Royal Society Open Science,* 5(3), 171712. DOI: 10.1098/rsos.171712

[31] Li, Z., Yu, L., Liu, Y., Sun, S. (2015). Efficient quantum dot-sensitized solar cell based on CdS_xSe_{1-x}/Mn-CdS/TiO_2 nanotube array electrode. *Electrochimica Acta,* 153, 200–209. DOI: 10.1016/j.electacta.2014.11.197

[32] Muthalif, M.P.A., Lee, Y.-S., Sunesh, C.D., Kim, H.-J., Choe, Y. (2017). Enhanced photovoltaic performance of quantum dot-sensitized solar cells with a progressive reduction of recombination using Cu-doped CdS quantum dots. *Applied Surface Science,* 396, 582–589. DOI: 10.1016/j.apsusc.2016.10.200

[33] Thanh, T.H., Lam, Q.V., Nguyen, T.H., Huynh, T.D. (2013). Performance of CdS/CdSe/ZnS quantum dot-sensitized TiO_2 mesopores for solar cells. *Chinese Optics Letters,* 11(7), 072501. DOI: 10.3788/COL201311.072501

[34] Chang, Y.-S., Choi, M., Baek, M., Hsieh, P.-Y., Yong, K., Hsu, Y.-J. (2018). CdS/CdSe co-sensitized brookite H:TiO_2 nanostructures: Charge carrier dynamics and photoelectrochemical hydrogen generation. *Applied Catalysis B: Environmental,* 225, 379–385. DOI: 10.1016/j.apcatb.2017.11.063

[35] Chang, Y.-S., Hsieh, P.-Y., Chang, T.-F.M., Chen, C.-Y., Sone, M., Hsu, Y.-J. (2020). Incorporating graphene quantum dots to enhance the photoactivity of CdSe-sensitized TiO_2 nanorods for solar hydrogen production. *Journal of Materials Chemistry A,* 8(28), 13971–13979. DOI: 10.1039/D0TA02359K.